AFRL-SR-BL-TR-00-

0093

REPORT DOCUMENTATION PAGE

1. AGENCY USE ONLY (*Leave Blank*)	2. REPORT DATE 20 Mar 2000	3. REPORT TYPE AND DATES COVERED Final Technical 15 Mar 96 through 14 Sep 99

4. TITLE AND SUBTITLE
Integrated Wavelength-Space-Time Optical Multiplexing Technologies and Architectures for Large-Scale, Reconfigurable, Multiple-Access Computer Networks

5. FUNDING NUMBERS
F49620-96-1-0077

6. AUTHORS
Julian Cheng

7. PERFORMING ORGANIZATION NAME(S) AND ADDRESS(ES)
University of New Mexico
Center for High Technology Materials
1313 Goddard SE
Albuquerque, NM 87106

8. PERFORMING ORGANIZATION REPORT NUMBER
FT - 1

9. SPONSORING / MONITORING AGENCY NAME(S) AND ADDRESS(ES)
Air Force Office of Scientific Research
Ballston Tower II
801 North Randolph Street
Arlington, VA 22203-1977

10. SPONSORING / MONITORING AGENCY REPORT NUMBER

11. SUPPLEMENTARY NOTES

12a. DISTRIBUTION / AVAILABILITY STATEMENT
UNL

12b. DISTRIBUTION CODE

13. ABSTRACT *(Maximum 200 words)*

Future computer networks will contain clusters of processors of various sizes that are interconnected over a wide range of distances, from dense local clusters to spatially distributed computer networks. To permit the simultaneous communication amongst many nodes, it will be necessary to develop practical networking technologies that provide multiple access, dynamic reconfigurability, and simultaneous communication through a shared channel. The objectives of this program are to investigate novel optical multiplexing architectures for interconnecting computer networks, and to develop their enabling technologies. To achieve these ends, we will investigate networks that combine wavelength, space, and time division multiplexing in new and different ways. For larger networks, new multiplexing techniques are needed that will use wavelength, space or time more efficiently, either by re-using the available channels or by combining several multiplexing platforms within a single network. These optical multiplexing techniques and their underlying technologies are the focus of the research program.

14. SUBJECT TERMS
Computer networks. optical multiplexing architectures

15. NUMBER OF PAGES
27

16. PRICE CODE
NSP

17. SECURITY CLASSIFICATION OF REPORT	18. SECURITY CLASSIFICATION OF THIS PAGE	19. SECURITY CLASSIFICATION OF ABSTRACT	20. LIMITATION OF ABSTRACT
	UNCLASSIFIED	UNCLASSIFIED	UNL

INTEGRATED WAVELENGTH-SPACE-TIME OPTICAL MULTIPLEXING TECHNOLOGIES AND ARCHITECTURES FOR LARGE-SCALE, RECONFIGURABLE, MULTIPLE-ACCESS COMPUTER NETWORKS

Julian Cheng, *Principal Investigator*

University of New Mexico, Center for High Technology Materials
1313 Goddard SE, Albuquerque, NM 87106
Phone: 505-272-7846; FAX: 505-272-7847
E-mail: cheng@chtm.unm.edu

FINALANNUAL REPORT (1997-1999)

for

CONTRACT #F49620-96-1-0077

from

THE AIR FORCE OFFICE OF SCIENTIFIC RESEARCH
BOLLING AIR FORCE BASE

DR. ALAN CRAIG, *Program Manager*

END DATE: November 15, 1999

1. Statement of Program Objective:

Future computer networks will contain clusters of processors of various sizes that are interconnected over a wide range of distances, from dense local clusters to spatially distributed computer networks. To permit the simultaneous communication amongst many nodes, it will be necessary to develop practical networking technologies that provide multiple access, dynamic reconfigurability, and simultaneous communication through a shared channel. The objectives of this program are to investigate novel optical multiplexing architectures for interconnecting computer networks, and to develop their enabling technologies. To achieve these ends, we will investigate networks that combine wavelength, space, and time division multiplexing in new and different ways. For larger networks, new multiplexing techniques are needed that will use wavelength, space, or time more efficiently, either by re-using the available channels or by combining several multiplexing platforms within a single network. These optical multiplexing techniques and their underlying technologies are the focus of this research program.

2. Review of Research Program

High speed gigabit-per-sec serial optical data links based on vertical-cavity surface-emitting lasers (VCSELs) have emerged from the laboratory and into the market place. But as the demand for bandwidth rapidly increases, system considerations limit the data bandwidth that can be transmitted through a single optical channel,. whose payload can be more effectively distributed through parallel optical links. While increasing the bus width (spatial parallelism) provides a straightforward means for increasing the data capacity, it also increases the cost of an interconnect. Moreover, variations in the electronic delay and fiber properties produce nonuniformity in latency and timing skew that limit the effective transmission distance of a parallel link. Fortunately, an optical link can multiplex many different data channels together in the wavelength regime to increase data capacity without increasing the physical bus width. Wavelength-division multiplexing (WDM) allows many parallel optical data channels to be multiplexed together and transmitted across large spatial distances on a single fiber, thus amortizing the cost of the interconnect over many different wavelength channels. At the destination nodes, individual data channels can be selected by using either a dispersive wavelength demultiplexer or by using a wavelength-selective REPD. To implement WDM technology at a local netrwork level requires the development of a cost-effective multiplexing and demultiplexing technology.

The simplest implementation of WDM is to use it as a passive means for sharing access to a physical interconnect medium (Fig. 1). In this straightforward implementation, WDM combines different wavelength channels and thus increases the data throughput in direct proportion to the number of multiplexible wavelengths. A number of wavelength-differentiated data channels can be multiplexed together using a monolithic VCSEL array in which the wavelength is graded in one dimension; the multiplexed data is then transmitted through a single optical fiber. At the opposite end of the optical interconnect, the multiplexed optical data may be broadcast to different

receivers, each of which selects an individual data channel using a wavelength-selective photodetector. In this approach, the distributed signal suffers a (-10 $\log_{10}$ N) optical fan-out loss, which limits the number of channels (N) that can be used. Alternatively, dispersive wavelength demultiplexers can be used to separate the wavelength channels in order to circumvent the optical fan-out loss, thus avoiding the use of wavelength-selective photodetectors. WDM can be a cost-effectieve approach for LANs if a simple means can be found for achieving multiple-wavelength VCSEL arrays in a controlled and reproducible manner. This paper describes the progress in the development of a simple technology for realizing uniformly wavelength-graded VCSEL and REPD arrays, and the experimental demonstration of a gigabit-per-sec WDM link based on these arrays.

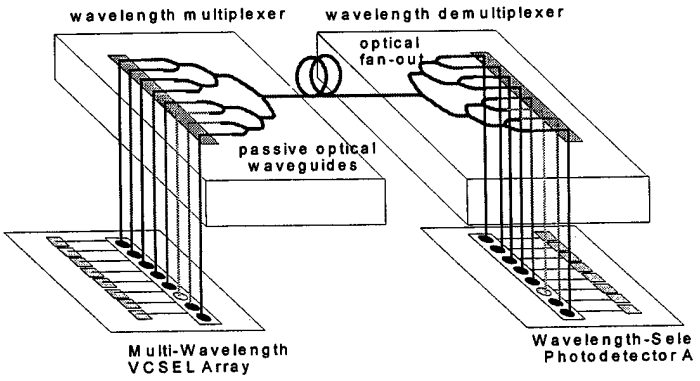

Figure 1. Schematic illustrating a wavelength-multiplexed parallel optical interconnect. Data from a multi-wavelength VCSEL array are multiplexed and transmitted through a single fiber, and is fanned out and demultiplexed at the other side by wavelength-selective photodetectors whose spectral photoresponse have matching wavelengths.

2.1. Wavelength Division Multiplexing using Wavelength-Graded VCSEL Arrays

To implement WDM at a local interconnect level requires a simple means for achieving multiple wavelength VCSEL arrays with a wide wavelength grading range in a controllable and reproducible manner, while achieving more uniform device characteristics within each array. One method for accomplishing these objectives is by locally controlling (scaling) the organometallic vapor phase epitaxial (OMVPE) growth rate of the VCSEL epilayers on a topographically patterned growth surface.[1,2] By perturbing the flow and concentration gradients of the reactant species, the growth rate can be locally enhanced or reduced,[3-5] resulting in a resonance structure whose layer thickness and resonance wavelength are scalable. Using this technique, we have previously achieved periodic wavelength-graded VCSEL arrays with a wavelength span of ~30nm and ~40 nm, respectively, using proton implant isolation[4] and selective wet oxidation[5] for current confinement, and demonstrated the repeatability of the wavelength grading range from array to array.

While most approaches for wavelength grading are based on varying the cavity length, our approach has been aimed at scaling the thicknesses of all the epilayers,

including the cavity length and both distributed-Bragg-reflector (DBRs) mirrors. By scaling the OMVPE growth rate of all the epilayers in a non-material-selective manner, the resonance wavelength can be controllably varied to achieve reduced (mirror) loss dispersion over the wavelength grading span. Varying the thickness of every layer in the entire epitaxial structure allows a spectral shift in the peak reflectance to track the change in the position of the lasing mode, thus reducing the wavelength dependence of the mirror loss by a factor of 3 over a 30 nm span (13% vs 35%). Combining this with a broadened gain spectrum results in more homogeneous lasing characteristics for all elements of a multi-wavelength VCSEL array. Since a smaller variation in optical loss results in a more uniform threshold gain across the wavelength-grading range, the potential exists for realizing arrays with more homogeneous lasing characteristics by scaling the growth rate of all the epi-layers in the VCSEL structure.

By controlling the surface topology, and using both the growth rate enhancement and reduction regimes, the emission spectra of a VCSEL array can be varied over a wide wavelength range. The growth rate, and thus the resonance wavelength of the VCSEL, depend on the aspect ratio of the surface features and on the spatial duty factor (SDF), which is defined as the ratio of the width of the ridge (+ sign) or the valley (- sign) to the spatial period p of the topological variations. The direct relationship between the resonance wavelength and these factors allows arrays with different wavelength spans to be designed.

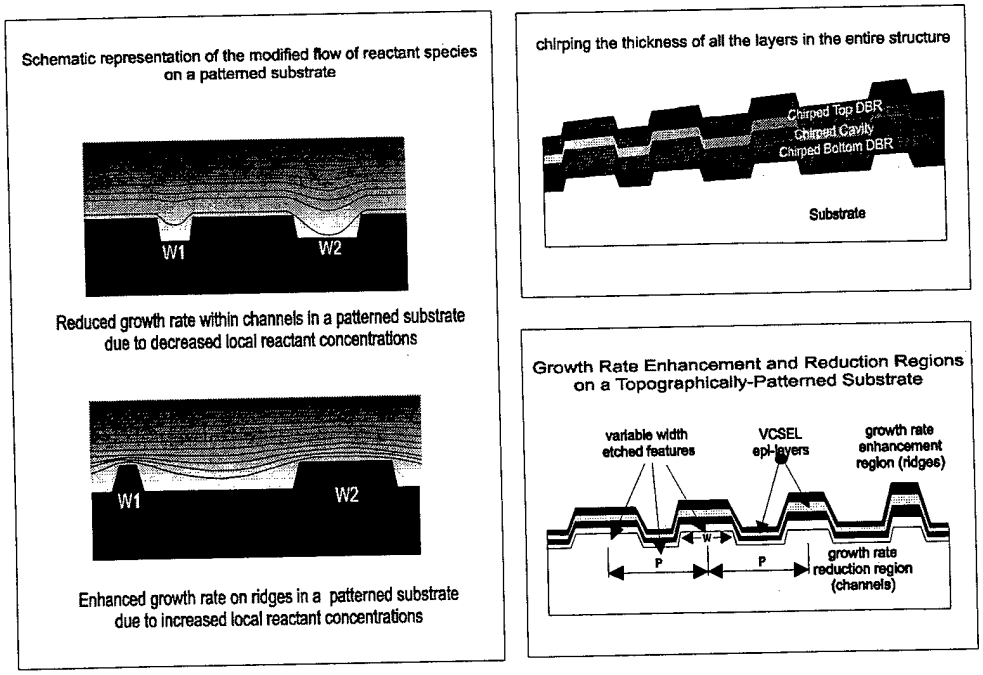

Figure 2. Modification of laminar flow on a topographically patterned substrate containing ridges and channels with a variable width, *w*, but a constant pitch, *p*, demonstrating the local enhancement and reduction of the MOCVD growth rate on ridges and channels, respectively.

2.1.1. Monolithic, Oxide-confined, Multiple-Wavelength VCSEL Arrays with a 57-nm Wavelength Grading Range

When wavelength-selective REPD's are used for wavelength demultiplexing[7], a 30-40 nm wavelength range provides at most 6 to 10 wavelength channels in the 850 nm and 980 nm wavelength regions, respectively. To increase the number of WDM channels, a wider wavelength grading range for cw lasing operation is required, which can be achieved by either reducing the optical loss dispersion across this wavelength range or by broadening the optical gain spectrum of the quantum wells (QW). We will show that the use of a selectively-oxidized upper distributed Bragg reflector (DBR) mirror with a flattened reflectance spectrum can reduce the loss dispersion to an a lower level ($\Delta\alpha_m$=14% variation in α_m over an 80 nm wavelength span) when all the epilayers are scaled. A more uniform optical loss, plus the higher optical gain that is afforded by strained $In_{0.2}Ga_{0.8}As$/GaAs quantum wells, made it possible to achieve room-temperature continuous-wave (cw) lasing of multiple wavelength VCSEL arrays with a 57 nm wavelength grading range.[6]

The VCSEL epilayer structure, which is described in Ref. 6, consists of a 1λ-thick active cavity containing four $In_{0.2}Ga_{0.8}As$/GaAs quantum wells, which is bounded on each side by a single AlGaAs/GaAs quarter-wave DBR pair, followed by a ¾λ-thick AlGaAs layer within which a 50 nm-thick oxidizable $Al_{0.98}Ga_{0.02}As$ current confinement layer is embedded. This entire structure is bounded below by a p-doped mirror consisting of 38.5 GaAs/AlGaAs quarter-wave DBR pairs, and above by the sequence of 3 GaAs/AlGaAs quarter-wave DBR pairs, an n-doped GaAs intracavity contact layer, and 4 selectively oxidized GaAs/AlO_x quarter-wave DBR pairs. All the AlGaAs/GaAs interfaces in each DBR mirror are linearly composition-graded.

The selectively-oxidized GaAs/AlO_x upper DBR mirror provides a larger index difference (Δn~2) and thus a smaller total thickness and a widened stop-band (800 nm to 1600 nm). It also results in a lower and more uniform optical mirror loss α_m over the 80-100 nm wavelength grading range compared to a conventional AlGaAs/GaAs upper DBR mirror. Moreover, the undoped GaAs/AlGaAs layers produce lower free carrier loss, α_{int},. The resulting lower total optical loss (α_m+α_{int}) makes it possible to achieve lasing over a wider wavelength range, while a reduced optical loss dispersion (smaller variations in α_m) leads to more uniform threshold gain and lasing characteristics. Figure 3 compares the variation of the calculated mirror loss (α_m) with wavelength over a 80 nm span for two wavelength-graded VCSEL structures, one (#1) containing two AlGaAs/GaAs semiconductor DBR mirrors, the other (#2) containing the same lower DBR mirror but a selectively oxidized upper AlO_x/GaAs DBR mirror. The thickness (*i.e.*, the growth rate) of each layer in both structures is scaled by the same factor, which allows a spectral shift in the peak reflectance to track the change in the resonance (lasing) wavelength for each VCSEL in an array. The results show both a lower total mirror loss and a significant (2.7×) reduction in mirror loss dispersion, with α_m changing by only 14% over a 80 nm wavelength range for the new design (#2), compared to 38.6% for the conventional VCSEL (#1). For comparison, the mirror loss dispersion of a VCSEL (#3) in which only the thickness of the active layer is graded is also shown,

which has a nearly ten-fold increase in α_m over the same 80 nm range. From Fig. 3, it is clear that the oxidized mirror provides the lowest loss dispersion, which should lead to a wider wavelength grading range.

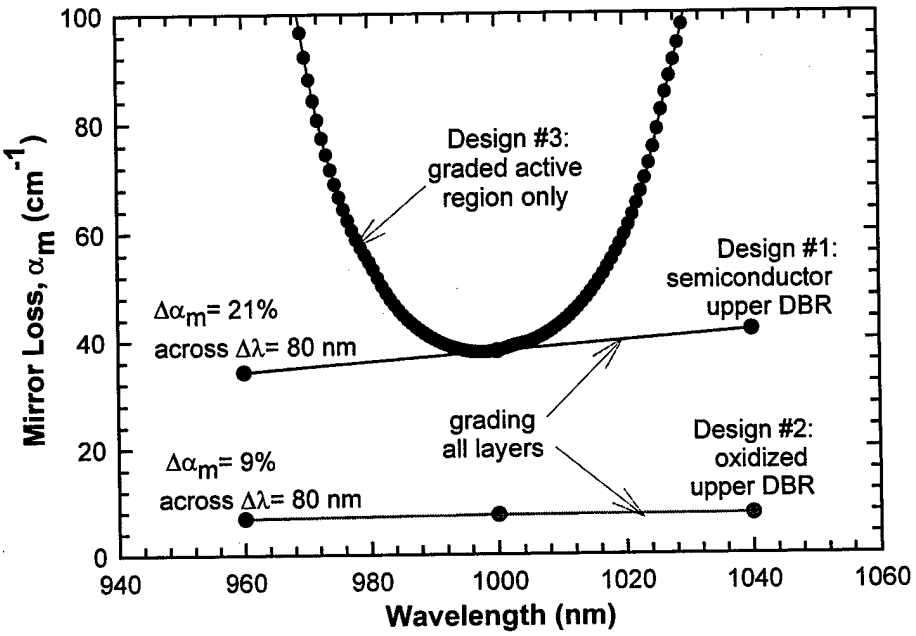

Figure 3. Comparison of the calculated optical mirror loss versus wavelength for three wavelength grading schemes for VCSELs. Designs 1 and 2 scale the thickness of all the epilayers, the former with two semiconductor DBR mirrors, the latter with an oxidized upper DBR .mirror. Design 3 grades only the thickness of the active region. Design 1 has the lowest optical loss and loss dispersion, and produced the widest wavelength grading range.

Fig. 4 shows the cw lasing wavelength (measured at ~1.1× I_{th}, at room temperature) as a function of the spatial duty factor for a linear array of VCSEL's with a 16 μm aperture. All elements of the array lased under cw operation with a wavelength grading span of 57 nm, ranging from 968 nm to 1025 nm. Very importantly, a relatively uniform wavelength gradient (*i.e.,* linear grading) has been achieved by carefully choosing the appropriate values of spatial duty factor during design of the pattern for the growth surface. The normalized cw lasing spectra of a single 18-element VCSEL array at room temperature are shown in Fig. 5, with a 57 nm wavelength grading range. The spectra are single-mode with a more than 20-dB side mode suppression ratio at bias currents up to ~1.3 × I_{th} except at the lower extreme of the grading range. The lasing linewidth of each element in the VCSEL array is ~ 0.18 nm.

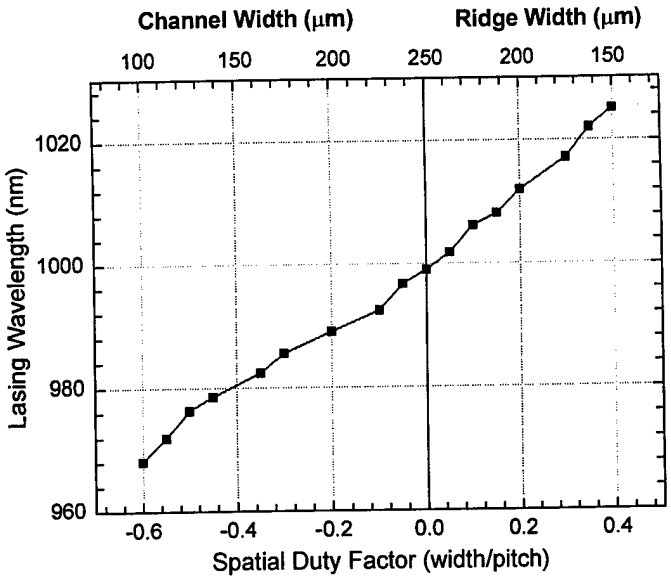

Figure 4. The cw lasing wavelength at room temperature as a function of the spatial duty factor for individual elements of a monolithic, oxide-confined, multi-wavelength VCSEL array (16-μm active area), which have a selectively oxidized upper DBR mirror and a 57-nm wavelength grading range.

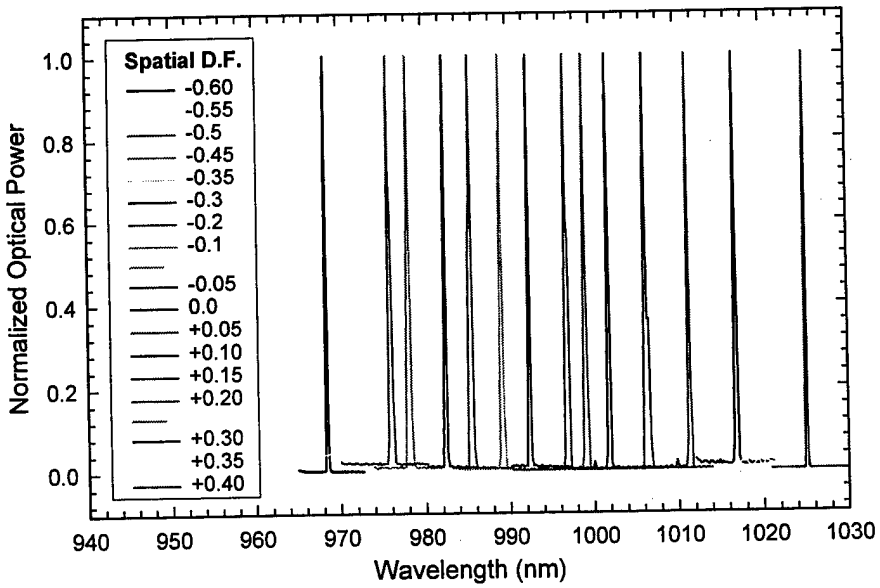

Figure 5. The normalized room-temperature, cw lasing spectra of a monolithic, wavelength-graded VCSEL array whose elements have a 16-μm oxide aperture and are biased at $1.1 \times I_{th}$. The single-mode lasing spectra are almost evenly spaced over a 57 nm wavelength span.

Fig. 5 shows the electrical and cw lasing characteristics of devices from a single multiwavelength VCSEL array at room temperature. The electrical characteristics are only weakly dependent on the spatial duty factor, with relatively uniform cw threshold currents (and voltages), which range from 4.5 ±1.5 mA (1.8 ±0.2 V). The intracavity n-contact allows the current to bypass the upper DBR mirror, resulting in a low series resistance (~45 Ω) and good voltage-vs-current characteristics, which are only weakly dependent on the spatial duty factor. However, the lasing characteristics show that at room temperature, the gain spectrum favors the longer wavelength devices (on ridges) over the shorter wavelength devices (in channels), with the former having higher peak powers than the latter. This shows that although the wavelength dependence of the optical loss has been reduced, the finite width of the optical gain spectrum can still produce nonuniform (albeit more uniform) lasing characteristics for arrays with a wide wavelength grading range.

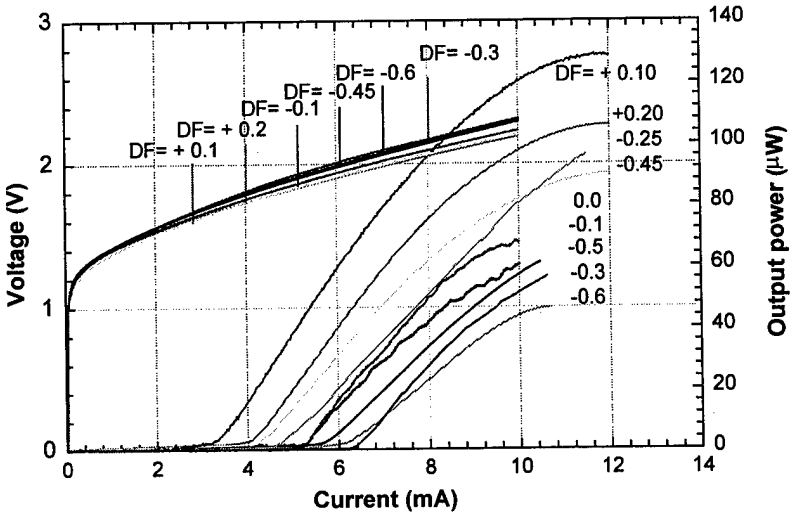

Figure 6. The light–vs-current (L-I), and voltage-vs-current (V-I) characteristics of VCSEL's from a wavelength-graded array under cw operation at room temperature, corresponding to different values of spatial duty factor spanning the wavelength grading range.

2.2. Resonance-Enhanced Wavelength-Selective Photodetector Arrays

Wavelength-graded VCSEL and REPD arrays can be monolithically integrated on a single epilayer structure grown on a patterned substrate to achieve closer wavelength matching between neighboring elements of the source and photodetector arrays.[6] Although the resonance cavity of a multi-quantum well VCSEL structure has excellent wavelength selectivity, it functions rather inefficiently as a wavelength-selective resonant photodetector. In order to achieve a high resonant absorption efficiency, it is necessary to remove an optimum number of DBR pairs from the upper mirror to broaden its photoresponse spectrum, thus trading off wavelength selectivity against the absorption efficiency. A wavelength-selective REPD can be integrated with a VCSEL on the same wafer.[9] The REPD is realized simply by removing an optimum number of DBR pairs from the upper mirror in selected areas of the

VCSEL wafer. Reducing the number of DBR pairs decreases the cavity Q value and increases the width of its resonance, allowing REPDs with a high absorption efficiency and a narrow spectral response to be achieved. The VCSEL and REPD thus share the same resonance cavity and the same lower DBR mirror, but differ in the number of DBR pairs in their respective upper mirrors. By sharing a common cavity and being in close proximity, the VCSEL and REPD have closely matched resonance wavelengths.

The signal rejection efficiency of individual REPDs is controlled by the width of its spectral response (Fig. 7); a narrow resonance also increases the number of wavelength channels that can be multiplexed. The peak absorption efficiency depends on the reflectivity of the upper DBR mirror (number of DBR pairs, N), and on the absorption coefficient $\alpha(\lambda)$ of the quantum wells, which varies with the resonance wavelength λ in a graded REPD array. The spectral width (FWHM) and the peak absorption efficiency both vary with N, which are plotted in Fig. 8 for a 980 nm VCSEL. The FWHM narrows with increasing N, achieving a peak efficiency of $\eta \approx 1$ at an optimum value of N*. This value is selected by a trade-off between the desired wavelength selectivity (the FWHM) and the absorption efficiency η of the REPD,[9] which is weighted over different values of $\alpha(\lambda)$ within the wavelength grading range in order to achieve optimum performance for the entire array. For 980 nm VCSELs, the peak absorption efficiency is achieved for N*=13, with a corresponding spectral FWHM of 2.0 nm. For 850 nm VCSELs, due to the differences in absorption, the optimum value of N* is 8 and the spectral width is $\Delta\lambda \approx 3.5$ nm.[9] The lower material absorption coefficient of the InGaAs quantum wells allows REPDs to be designed with a narrower wavelength selectivity (2.0 nm FWHM, vs 3.5 nm for GaAs) while retaining a high peak absorption efficiency (> 90%). The narrower wavelength selectivity leads to a reduction of the optical crosstalk between channels, thus allowing more wavelength channels to be used within a given spectral band.

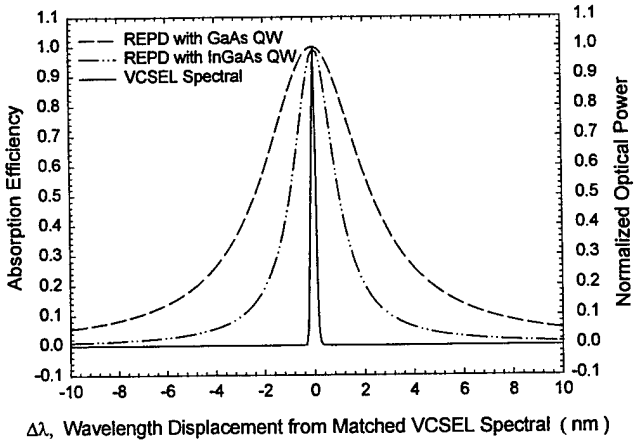

Figure 7. A comparison of the wavelength selectivity of REPD's containing GaAs quantum wells and strained InGaAs quantum wells using their calculated absorption efficiency spectra, each centered with respect to the lasing spectrum of a wavelength-matched VCSEL.

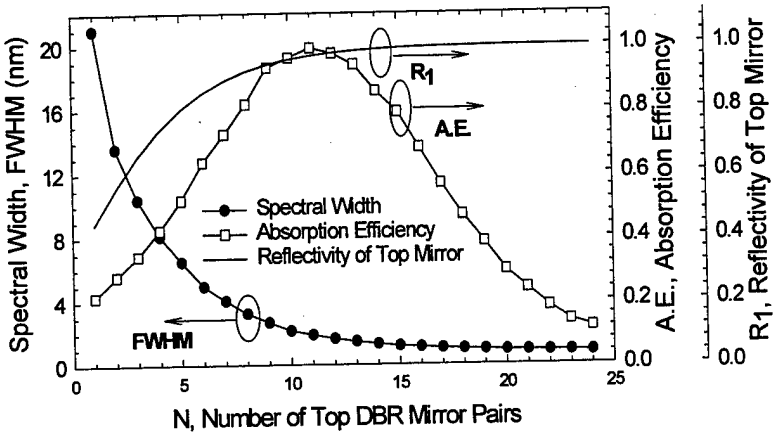

Figure 8. The dependence of the peak absorption efficiency and the spectral width (FWHM) of the photoresponse of a REPD on the number of DBR pairs and on the reflectivity of the upper mirror. The REPD contains 4 InGaAs quantum wells and was designed for operation at 980 nm.

2.3. Quasi-Planar Monolithic Integration of High-Speed VCSEL and REPD Arrays

In order to achieve a higher modulation speed, a quasi-planar technology[10-12] has been developed for the monolithic integration of oxide-confined VCSEL and REPD arrays. These high speed devices are fabricated using an approach in which the oxide current aperture is formed by concatenating a number of discrete crescent-shaped oxidation fronts emanating from a local pattern of etched trenches (Fig. 9).[10] This approach preserves the planarity of the wafer while improving the dimensional control for devices with very small oxide apertures (<4 μm). Selective oxidation for current confinement presents a problem for the monolithic integration of VCSEL and REPD arrays due to the disparate size requirements of the current apertures for the VCSEL (<10 μm) and the REPD (>30 μm), which share a common epilayer structure. The VCSELs and REPDs are typically isolated mesa structures from whose periphery selective lateral oxidation proceeds. For VCSELs the oxidation length is chosen as a trade-off between the accuracy of the final oxide aperture and the need for a low contact resistance, and is typically 10-20 μm. As a result of this oxidation length, the concomitant lateral oxidation of the larger REPD mesas produces a large parasitic capacitance that reduces the bandwidth of the photoresponse. It is thus desirable to develop a new oxidation technique for monolithic integration that can accommodate a range of different oxide apertures with arbitrary geometries while improving dimensional control, preserving planarity, and minimizing device parasitics. This has been achieved using a variant of the etched-trench

oxidation technology described in Ref. 11 and Ref. 12, which resulted in quasi-planar, high-speed VCSEL and REPD arrays with oxide dimensions as small as 2 μm.

In the monolithic integration of dense arrays, the size of the etched mesa (EM) is determined not only by the desired electrical and thermal characteristics, but also by the requirements of dense array integration. To minimize the power dissipation in dense arrays, devices with a small oxide aperture are needed, but due to limits in the accuracy of the oxidation rate, very small micro-cavities cannot be accurately and reliably achieved without reducing the mesa size and oxidation length, which increases the electrical and thermal resistances. For a given process control accuracy, the percentage error in the dimension of the oxide aperture can become unacceptably high when the final dimension is small compared to the total oxidation length. The oxidation length (and time) can be reduced without reducing mesa size or sacrificing planarity by the introduction of local oxidation centers such as etched holes,[11-12] from which multiple oxidation fronts can proceed to define an enclosed oxide aperture (Fig. 11). Arbitrary oxide aperture geometries can be defined using discrete etched holes,[11,12] or alternatively by using linear or crescent-shaped segments of etched trenches (Fig. 10),[10] from which oxide fronts as narrow as 2 μm can be concatenated to form a single continuous aperture (Fig.11). By not removing all of the surrounding semiconductor material, planarity is maintained while the thermal resistance is decreased to alleviate thermal roll-over.

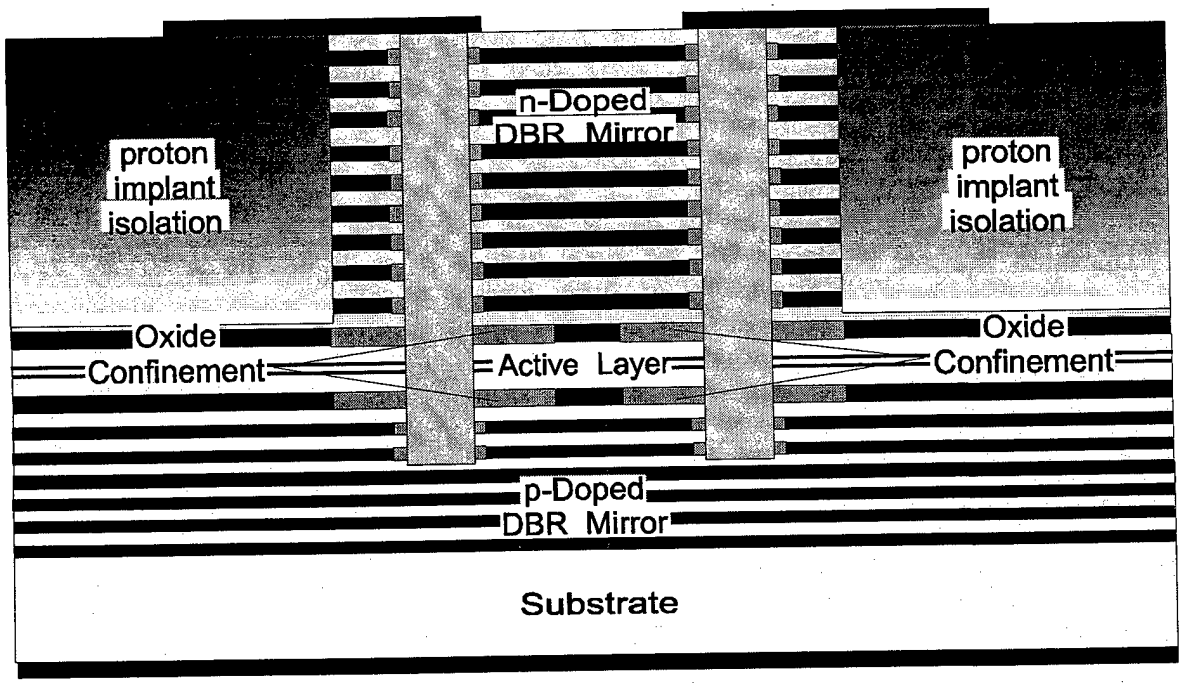

Figure 9. The schematic design and epitaxial layout of a quasi-planar technique which uses a local pattern of etched trenches to achieve an oxide front with arbitrary geometry with improved dimensional control over the oxide aperture. Implantation is also used to isolate the active area in this planar strcuture.

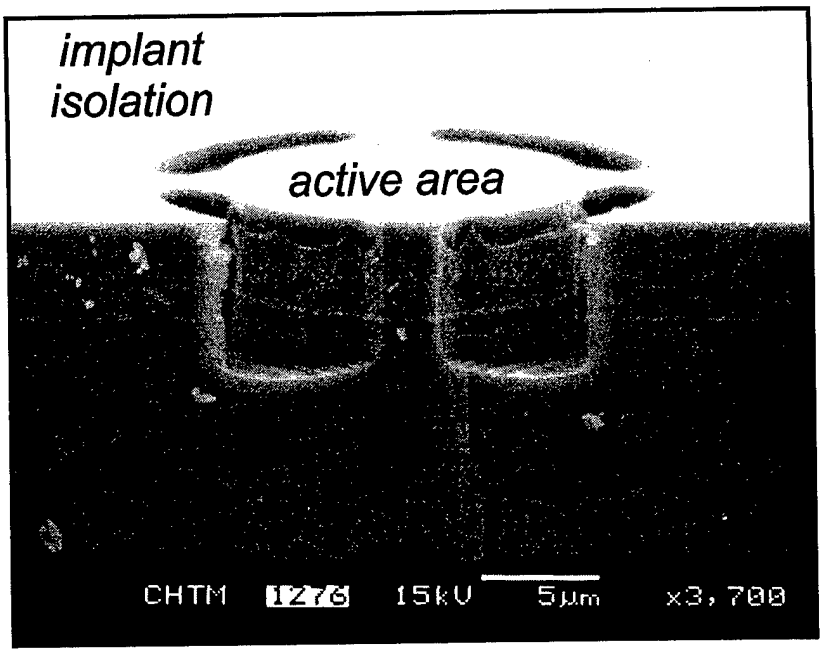

Figure 10 Scanning electron microscope (SEM) photo showing the profile of the etched trench segments and the local oxidation fronts.

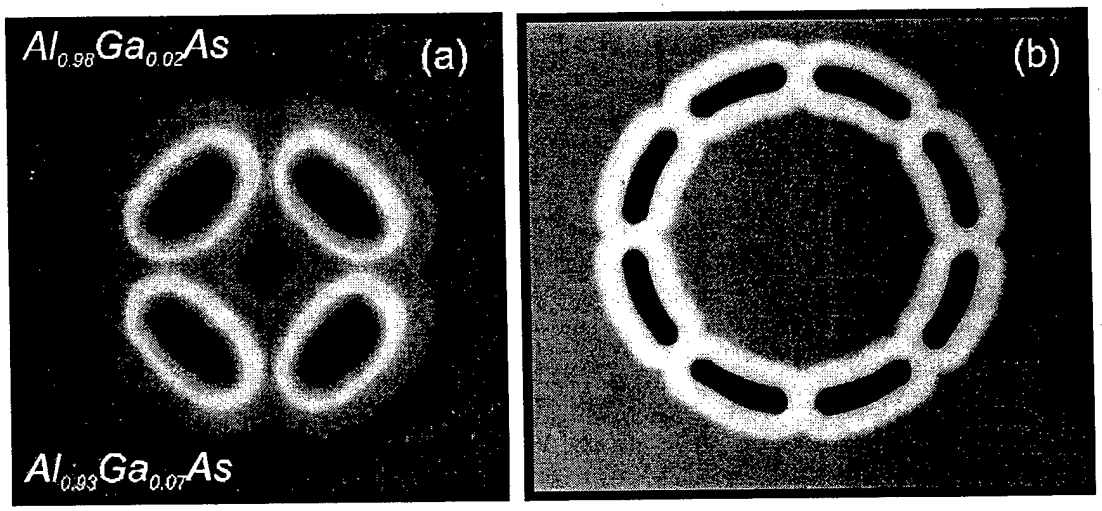

Figure 11. SEM photographs showing the formation of a continuous oxide front by concatenatring the local oxidation fronts (~3 µm wide) emanating from several discrete crescent-shaped segments for: (a) a VCSEL with a 2 µm aperture, and (b) an REPD with a 20 µm aperture.

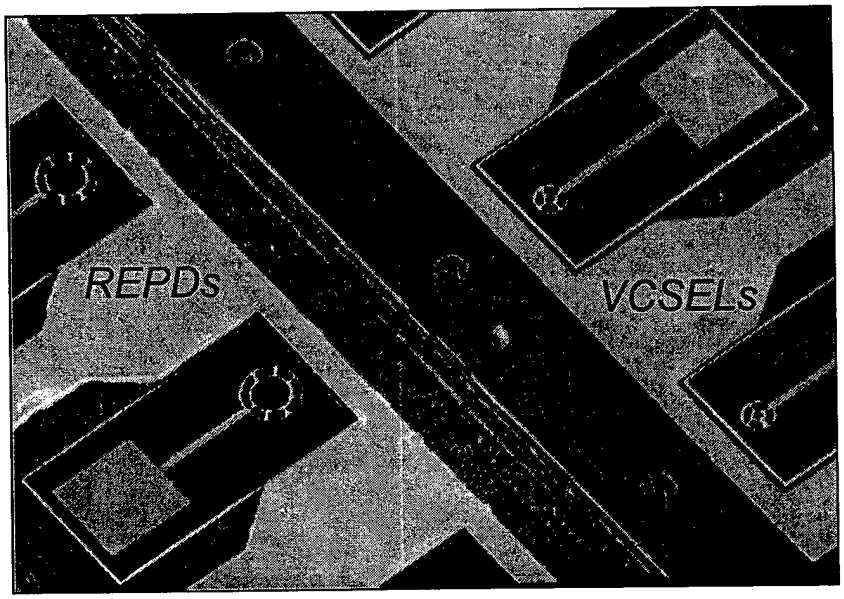

Figure 12. SEM photograph showing quasi-planar monolithic arrays of high-speed VCSELs and REPDs with closely matching resonance wavelengths.

This technique has been applied to the quasi-planar integration of monolithic VCSEL and REPD arrays.[10] Several crescent-shaped segments are etched into a planar wafer (Fig. 10) to allow selective wet oxidation to locally define the oxidation fronts that delineate the active area of the VCSEL or REPD. The number of segments is increased with larger oxide aperture size (4 for VCSELs and 8 for REPDs) in order to provide uniform current spreading from regions lying outside the circular trenches. After oxidation, the surrounding areas are bombarded with a multi-level proton implant for device isolation (Fig. 9). All of the devices were designed to have coplanar strip lines in order to evaluate their high speed response. Figure 12 shows the monolithic integration of VCSEL and REPD arrays using the etched trench (ET) approach.

An important advantage of the planar ET technique is that since the oxidation length is decreased to 2-3 μm, more precise control of the final aperture can be achieved, especially for devices with small active areas (<4 μm). For an etched mesa (EM) device with a 2 μm active region and a 10 μm oxidation length, an uncertainty in the oxidation rate of ± 5% would lead to an uncertainty of ± 0.5 μm (25%) in the active area diameter. For an ET VCSEL with a reduced oxidation length of 2 μm, the uncertainty in the aperture size is only ± 0.1 μm (5%), a five-fold improvement.

Figure 13 compares the dc electrical and lasing characteristics of two 10-element VCSEL arrays with an active area diameter of 2 μm, fabricated by the planar and mesa approaches using the same wafer,. The characteristics of the two types of devices are similar, with the planar devices showing much better uniformity. All devices have low threshold voltages (1.45 V to 1.60 V) and low threshold currents (≈0.9 mA). One notable difference between the ET VCSELs and EM VCSELs is that although both have comparable peak optical

output powers (0.7 mW for 2 μm devices), thermal roll-over occurs at a much higher current for the former.

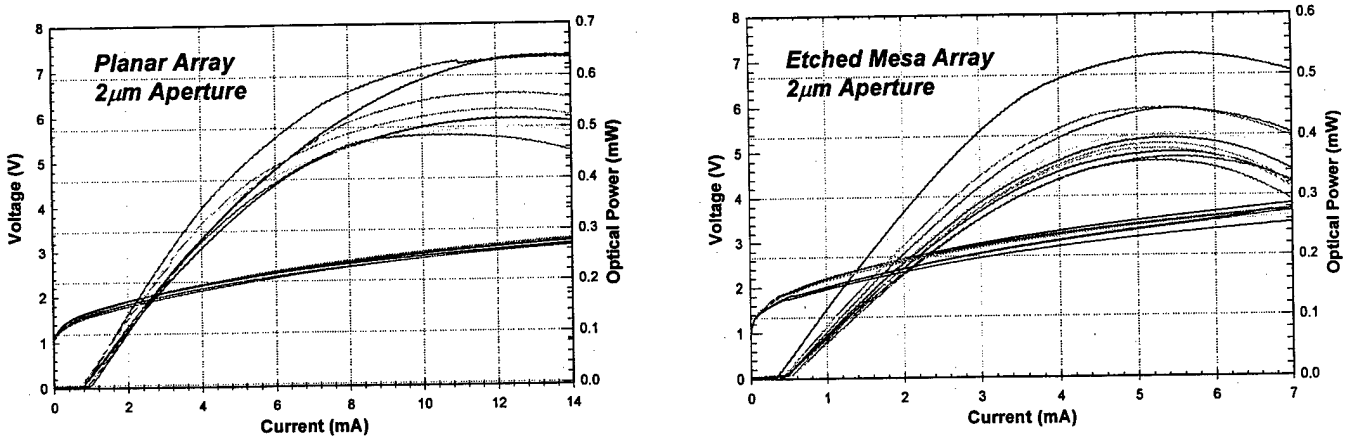

Figure 13. A comparison of the room-temperature electrical and cw lasing characteristics of of monolithic VCSEL arrays with oxide apertures of 2 μm, fabricated by using the quasi-planar approach (left) and the conventional etched mesa approach (right).

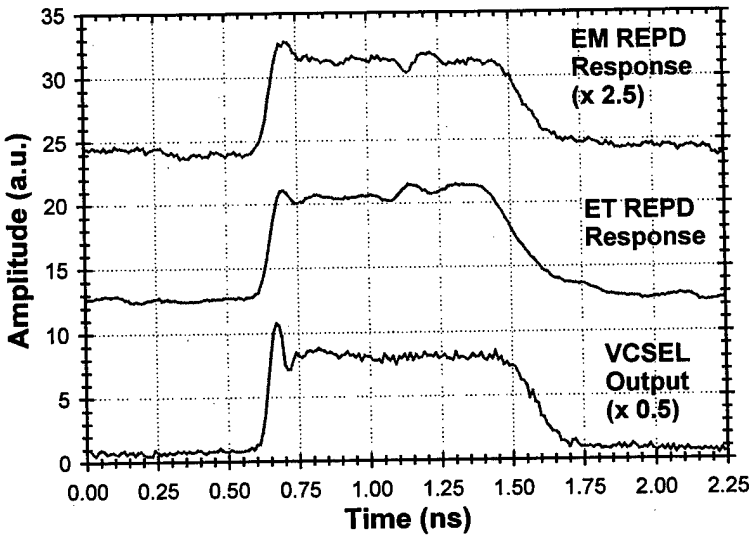

Figure 14. The photoresponse of a REPD fabricated by the mesa approach (upper trace) and the planar approach (lower trace) to a 1 ns wide optical pulse from a quasi-planar VCSEL (lower trace) with a matching wavelength, showing a rise time of ~ 65 ps.

The high speed modulation characteristics of the planar and etched mesa VCSELs are compared in Fig. 14 and Fig. 15. The large-signal photoresponse of REPDs with a 30 μm optical aperture in response to the optical modulation

from a 6 μm VCSEL source (Fig. 14) shows a 10-90% rise time of ~ 65 ps for both devices. Figure 14 compares the small-signal modulation bandwidth of the planar and etched-mesa VCSELs (~6 μm aperture) as a function of normalized bias current. At low bias current levels the f_{3dB} frequencies are identical, but as the bias current increases the EM devices show a slightly higher speed, with a maximum frequency of 13.5 GHz vs 11.8 GHz.

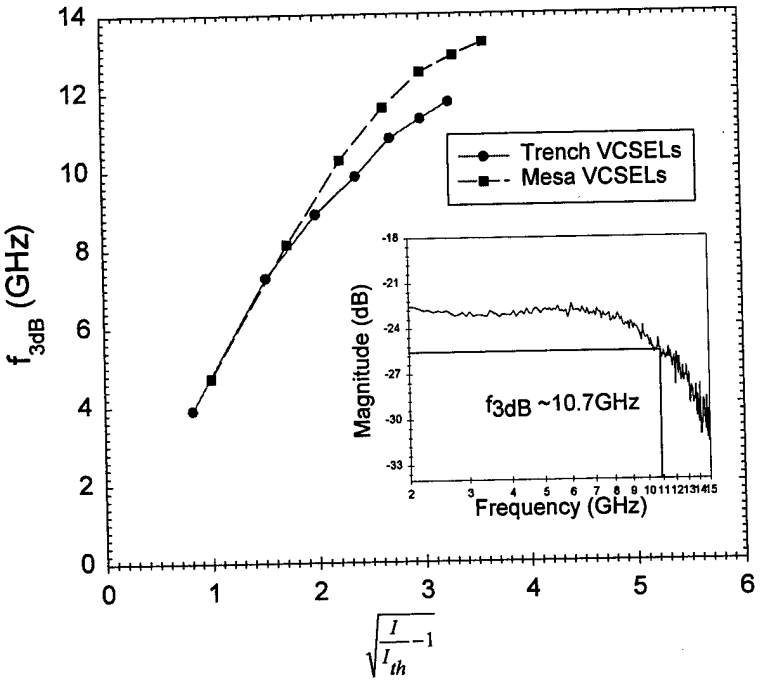

Figure 15. Comparison of f_{3dB} (-3dB frequency of $|S_{21}|$) for two VCSELs with a 6 μm oxide aperture fabricated by the quasi-planar approach and the etched mesa approach, respectively, as a function of the square root of the normalized dc bias current above threshold. Inset: $|S_{21}|$ curve of an etched trench VCSEL at $I = 9*I_{th}$.

2.4. Optical Crosstalk in a WDM Link

The wavelength selectivity of an REPD, or the optical crosstalk between adjacent WDM channels, depends on the spectral width of its photoresponse. A narrower width results in greater wavelength selectivity and lower optical crosstalk between channels, allowing more closely spaced wavelength channels to be used within a given spectral band. The use of GaAs QWs in the earlier WDM link[13] led to a non-optimum trade-off between the absorption efficiency of the REPD and its wavelength discrimination ability (~4 nm), resulting in significant variations in the responsivity across the wavelength grading range. The use of strained InGaAs QWs produces better optimized REPD arrays with an improved wavelength selectivity (~2 nm), higher absorption efficiency (>90%), and a more uniform responsivity. For two neighboring WDM channels with a fixed 4 nm wavelength spacing, the 980 nm REPD has a

higher optical discrimination ratio (16.5:1) than the 850 nm REPD (3.8:1), see Fig. 16. As shown in fig. 7, the measured photoresponse spectra of a 850 nm REPD and a 980 nm REPD show a FWHM of 4 nm and 2 nm, respectivity.

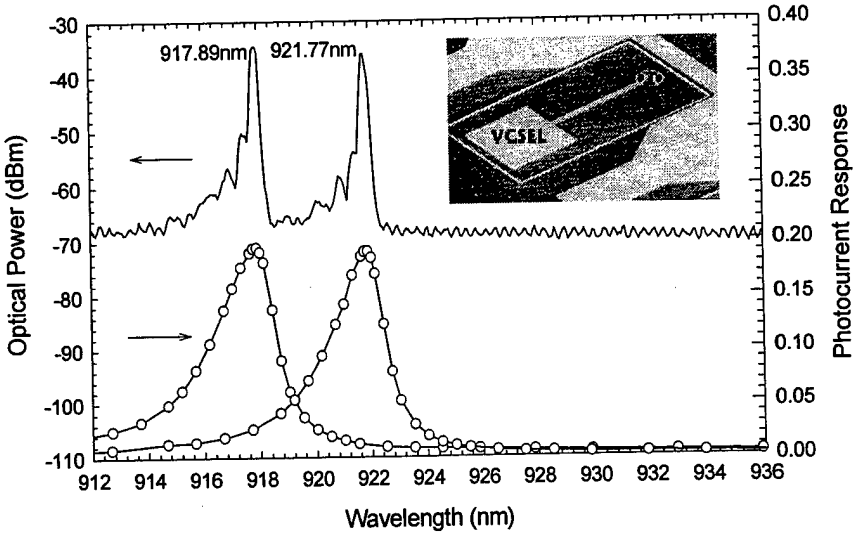

Figure 16. The lasing spectra of two wavelength-multiplexed VCSEL channels with a 3.9 nm wavelength separation (upper trace), and the photoresponse spectra of two REPDs with matched resonance wavelengths (lower trace). The inset shows SEM photomicrographs of a quasi-planar VCSEL (above) and a REPD (below) fabricated using the etched-trench approach for oxide confinement.

The VCSEL's and REPD's used in the WDM experiments are quasi-planar, oxide-confined devices. The VCSELs have a 6 μm active area and a small-signal modulation bandwidth of >10 GHz , while the REPD's large-signal photoresponse has a rise time of 65 ps. The optical crosstalk between different wavelength channels, or equivalently the channel selectivity, has been characterized under large signal modulation conditions. The upper trace in Fig. 16 shows the cw lasing spectra of two VCSELs from a monolithic array whose center wavelengths (917.9 nm and 921.8 nm) are separated by 3.9 nm, while the lower trace shows the photoresponse spectra of two wavelength-matched REPD's from a neighboring array with matching wavelengths. The modulated optical outputs of the VCSELs are multiplexed together by a fiber coupler, and then transmitted to the REPDs through an optical fiber. The dc response of each REPD shows an asymmetric photocurrent spectrum with a FWHM of 2.5 nm, and he dc optical crosstalk from neighboring channels is –12.2 dB for the 917.9 nm REPD, and is –8.4 dB for the 921.8 nm REPD.

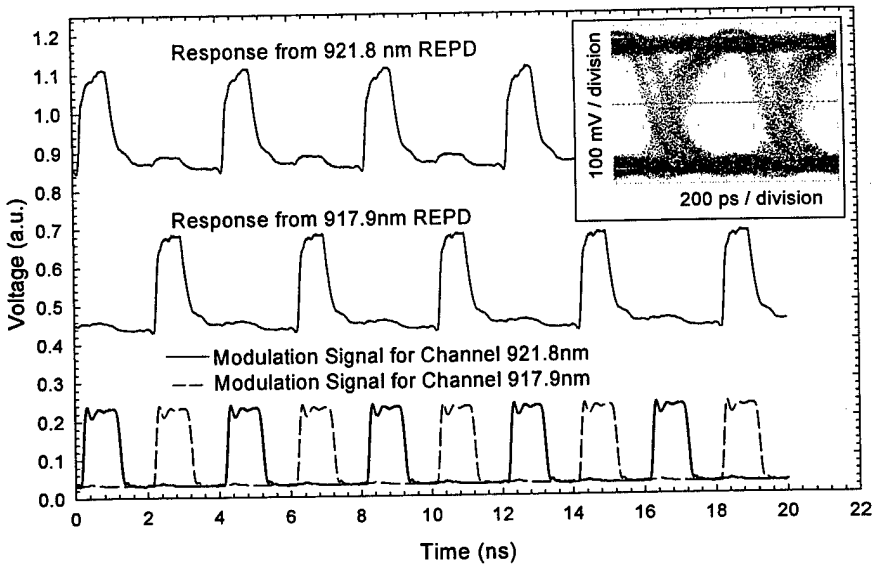

Figure 17. Demultiplexed signals (upper traces) from two wavelength-matched REPDs in response to the optical input signal from two wavelength-multiplexed, high-speed data channels with a wavelength separation of $\Delta\lambda \sim 3.9$ nm. Each channel is modulated by one of the two non-overlapping, 500 Mb/s RZ, 1 ns pulse patterns shown in the lower trace. Inset shows the 1.25 Gb/s eye diagram measured by a REPD-based optical receiver in response to illumination by a multiplexed optical signal at a BER of $< 10^{-11}$.

2.5. High-Speed Wavelength Division Multiplexing and Demultiplexing using Monolithic VCSEL and REPD Arrays

The optical crosstalk was also measured under large-signal data modulation conditions The VCSELs were biased at lightly below threshold and were separately modulated using two temporally non-overlapping 500 Mb/s RZ (return-to-zero) data patterns consisting of 1 ns wide pulses (which is equivalent to a 1 Gb/s NRZ data stream). Their optical outputs were combined (wavelength multiplexed) and transmitted through a single optical fiber, and the response of each REPD to the multiplexed optical data stream is individually measured to demonstrate demultiplexing using a wavelength-selective photodetector. The lower time trace in Fig. 17 shows the two temporally-displaced and non-overlapping modulation signals of the VCSELs, while the two upper traces show the demultiplexed photoresponse of the two REPD's. The weaker pulses in each trace represent the photoresponse of each REPD to the optical data at the nonresonant wavelength, *i.e.,* the optical crosstalk level, which is –10.4 dB for the 917.9 nm REPD, and is –8.2 dB for 921.8 nm REPD. The inset of figure 17 shows a 1.25 Gb/s eye-diagram for the demultiplexed signal of the matched wavelength channel obtained under conditions for achieving a bit error rate (BER) of $<10^{-11}$. High-speed wavelength demultiplexing has thus been achieved by this simple WDM link at a data rate of 1.25 Gb/s, which is limited by the speed of the receiver (including the REPD).

2.6. A 1 Gb/s WDM Optical Link Demonstration

In the experimental WDM setup, these VCSELs are independently modulated by two pseudorandom data pattern generators synchronized by a common clock module. The optical output of each VCSEL is butt-coupled to a lensed single-mode fiber (SMF), multiplexed using a 2 ×1 fiber coupler and transmitted through a 1 km-long SMF. At the receiver end the multiplexed signal is fanned-out and distributed to each receiver via a 1×2 coupler (with a 3 dB optical fan-out loss), where each channel is selected by an REPD with the appropriate wavelength.

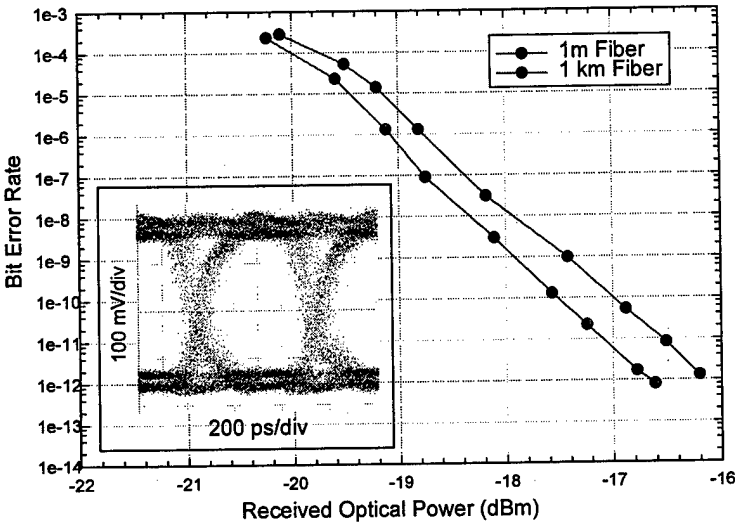

Figure 18. BER versus received optical power at 1Gb/s with respect to 1 meter fiber length and 1 km fiber length. The inset shows the eye diagram after 1 km transmission, with a BER at 10^{-12}.

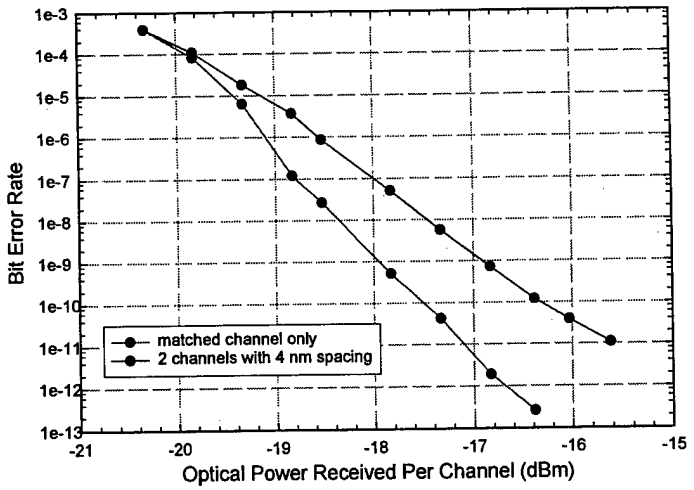

Figure 19. BER versus received optical power at 1 Gb/s for: (a) single matched-channel operation, and (b) demultiplexing the optical data from two multiplexed WDM channels 4 nm apart.

Figure 18 shows the BER performance of a single-channel VCSEL/REPD link with matching wavelengths at 1 Gb/s, with a link span of 1m and 1km, respectively. For the shorter link, the REPD-based receiver achieved a BER of 10^{-12} at an average optical power of –16.7 dBm. The receiver sensitivity was degraded in part by the responsivity of the REPD and the finite extinction ratio of the VCSEL. Taking all sources of noise current into account at the input, the calculated receiver sensitivity is –17.0 dBm at 1 Gb/s, which is close to the experiment result of –16.7 dBm. The BER performance for the longer (1 km) link shows a similar shape as the shorter (1m) link, except for a 0.5 dB power penalty. The inset of Fig. 18 shows the eye-diagram at BER=10^{-12} ($\eta\langle P\rangle$=-16.9 dBm).

The power penalty due to the optical crosstalk from each neighboring wavelength channel (±4 nm away) has been determined by comparing the bit error rate (BER) in the absence and the presence of the second channel (Fig.19). Due to optical crosstalk, the received signal power level in the matched channel must be raised in order to achieve the same BER and signal-to-noise level (S/N). For a REPD with a signal rejection ratio of 10 dB for the neighboring channel, the crosstalk produces a "noise" current equal to 10% of the signal photocurrent. The calculated signal level needed to achieve a 10^{-9} BER is –17.0 dBm, compared to –16.9 dBm measured. The calculated power penalty for interchannel optical crosstalk is 1 dB for BER=10^{-9} and 1.5 dB for BER=10^{-11}. Since the crosstalk level is fixed, the power penalty increases with decreasing BER (*i.e.,* increasing S/N ratio). The optical crosstalk level rolls off rapidly with wavelength separation, the contributions to crosstalk from the wavelength channels that are further away ($\Delta\lambda \geq \pm 8$ nm for the next nearest channels) are negligible.

An important issue that must be addressed in the use of wavelength-selective REPDs for DEMUX operations in a WDM link is the effect of wavelength mismatch between the VCSEL and REPD spectra on the latter's photoresponse. Mismatch may result from either fabrication tolerances and growth variations, or from the thermally-induced wavelength de-tuning caused by ambient temperature variations. The effect of wavelength de-tuning on the BER performance of a matched link needs to be quantitatively studied. For a four-channel WDM link, there is also a 6 dB optical fan-out loss plus a 2.0 dB crosstalk power penalty, whose effect could be comparable to that of wavelength detuning. Either the fanout loss or the detuning penalty can consume most of the system's power margin and limit the link span, and therefore cannot co-exist. Either dispersive wavelength demultiplexing or temperature compensation (or wavelength adjustment) would be required.

2.7. Conclusions

In conclusion, we have described a monolithic technology for realizing multi-wavelength arrays of VCSELs and REPDs with matching wavelengths over a span of yp to 57 nm. We have also described a quasi-planar technique for integrating high-speed, oxide-confined VCSEL and REPD arrays with an arbitrary oxide geometry by etching a pattern of local oxdiation centers into the planar epilayer substrate. We

have also demonstrated a 1 Gb/s-per-channel optical WDM link in which the outputs of a monolithic multiple-wavelength VCSEL array are multiplexed into a single fiber, transmitted through a 1 km SMF, and then demultiplexed by using wavelength-matched REPD-based receivers. The modulation speed can be improved by using a faster receiver and optimizing the REPD's photoresponse.

2.8. References:

1. P. Demeester, P. Van Daele, and R. Baets, "Growth behavior during non-planar metalorganic vapor phase epitaxy," *Journal of Applied Physics*, vol. 63, no. 7, pp. 2284-2290, 1988.
2. L. Buydens, P. Demeester, M. Van Ackere, A. Ackaert and P. Van Daele, "Thickness variations during MOVPE growth on patterned substrates," *Journal of Electronic Materials*, vol. 19, no. 4, pp. 317-321, 1990.
3. F. Koyama, T. Mukaihara, Y. Hayashi, N. Ohnoki, N. Hatori, and K. Iga, "Wavelength control of vertical cavity surface-emitting lasers by using nonplanar MOCVD", IEEE photon. Technol. Lett., vol. 7, pp. 10-12, 1995.
4. G. G. Ortiz, S. Q. Luong, S. Z. Sun, and Julian Cheng, H. Q. Hou, G. A. Vawter, and E. Hammons: "*Monolithic, Multiple Wavelength Vertical-Cavity Surface-Emitting Laser Arrays by Surface-Controlled MOCVD Growth Rate Enhancement and Reduction*", IEEE Photonics Technol. Lett., Vol. 9, No. 8, pp. 1069-1071; August 1997.
5. Yuxin Zhou, S. Luong, C.P. Hains, and Julian Cheng: "*Oxide-Confined Monolithic, Multiple-Wavelength Vertical-Cavity Surface-Emitting Laser Arrays with a 40 nm Wavelength Span*", IEEE Photonics Technol. Lett., Vol. 10, 1998.
6. S. Q. Luong, G. G. Ortiz, Y. Zhou, Jun Lu, C. P. Hains, Julian Cheng, H. Q. Hou, and G. A. Vawter: "*Monolithic, Wavelength-Graded VCSEL and Resonance-Enhanced Photodetector Arrays for Parallel Optical Interconnects*", IEEE Photonics Technol. Lett., Vol. 9, No. 5, pp. 642-644, May, 1998.
7. Kai Yang, Yuxin Zhou, X. D. Huang, C.P. Hains, and Julian Cheng, "Monolithic, Oxide-confined, Multiple-Wavelength Vertical-Cavity Surface-Emitting Laser Arrays with a 57-nm Wavelength Grading Range using an Oxidized Upper Bragg Mirror", IEEE Photonics Technol. Lett., vol. 12, no. 3, 2000.
8. G. G. Ortiz, C. P. Hains, Julian Cheng, H. Q. Hou, and J. C. Zolper, *"Monolithic integration of $In_{0.2}Ga_{0.8}As$ vertical-cavity surface-emitting lasers with resonance-enhanced quanum-welll photodetectors*", Electronics lett., Vol. 32, No. 13, pp. 1205-1207, June 1996.
9. Julian Cheng, S. Q. Luong, Y.-X. Zhou, A. C. Alduino, Jun Lu, C. P. Hains, H. Q. Hou, B. E. Hammons, G. A. Vawter: "*Monolithic wavelength-graded VCSEL and wavelength-selective photodetector arrays for wavelength-division-multiplexed optical interconnect applications,* SPIE Proceedings, Vol. 3288, "Optoelectronics Interconnects and Packaging V", pp. 2-9, Jan. 1998.
10. A. C. Alduino, S. Q. Luong, Yuxin Zhou, C. P. Hains, and Julian Cheng, " Quasi-Planar monolithic integration of high-speed VCSEL and resonant enhanced photodetector arrays" *IEEE Photon. Technol. Lett., vol. 11, pp.512-514, May 1999.*

11. R. P. Schneider Jr. "A new planar Laser". IEEE Spectrum vol.35, no. 2, pp.52-53, 1998.

12. C. L. Chua, R. L. Thornton, and D. W. Treat, "Planar laterally oxidized vertical-cavity lasers for low-threshold high-density top-surface-emitting arrays," IEEE Photon. Technol. Lett., vol. 9, no. 8, August 1997.

13. A. C. Alduino, S. Luong, Y. Zhou, C. P. Hains, and J. Cheng, " Wavelength multiplexing and demultiplexing using multi-wavelength VCSEL and resonant-enhanced photodetector arrays" *IEEE Photon. Technol. Lett., vol.10, pp.1310-1312, Sept.1998.*

3. Research Personnel

This work was performed primarily by members of Professor Julian Cheng's optoelectronics group at the University of New Mexico's Center for High Technology Materials. The contributing researchers included graduate students Gerry Ortiz, Yuxin Zhou, A. C. Alduino, Sanh Q. Luong, Kai Yang and Lei Yang, plus research engineer C. P. Hains, and MOCVD crystal grower Nelson Li.

4. Publications

4.1. Refereed Journal Papers

1) G. G. Ortiz, C. P. Hains, Julian Cheng, H. Q. Hou, and J. C. Zolper, *"Monolithic integration of $In_{0.2}Ga_{0.8}As$ vertical-cavity surface-emitting lasers with resonance-enhanced quanum-welll photodetectors"*, Electronics lett., Vol. 32, No. 13, pp. 1205-1207, June 1996.

2) G.G.Ortiz, C. P. Hains, Julian Cheng, J. C. Zolper, "*Efficient cryogenic VCSELs with chirped multi-quantum-wells with a wide operating temperature range*", IEEE Photonics Technol. Lett., Vol. 8, no. 10, October 1996.

3) G. G. Ortiz, S. Q. Luong, S. Z. Sun, and Julian Cheng, H. Q. Hou, G. A. Vawter, and E. Hammons: "*Monolithic, Multiple Wavelength Vertical-Cavity Surface-Emitting Laser Arrays by Surface-Controlled MOCVD Growth Rate Enhancement and Reduction",* IEEE Photonics Technol. Lett., Vol. 9, No. 8, pp. 1069-1071; August 1997.

4) G. G. Ortiz , C. P. Hains, S. Luong, S. Z. Sun, Julian Cheng, H. Q. Hou, G. A. Vawter and B. E. Hammons: *"Multiple Wavelength Vertical-Cavity Surface-Emitting Laser Arrays using Surface-Controlled MOCVD Growth Rate Enhancement and Reduction",* OSA Trends in Optics and Photonics (TOPS), Vol. 15: Advances in Vertical-Cavity Surface-Emitting Lasers, edit. C.Chang-Hasnain, pp. 29-35, Sept. 1997.

5) S. Q. Luong, G. G. Ortiz, Y. Zhou, Jun Lu, C. P. Hains, Julian Cheng, H. Q. Hou, and G. A. Vawter: "*Monolithic, Wavelength-Graded VCSEL and Resonance-Enhanced Photodetector Arrays for Parallel Optical Interconnects",* IEEE Photonics Technol. Lett., Vol. 9, No. 5, pp. 642-644, May, 1998.

6) Alduino, Yuxin Zhou, S. Luong, C. P. Hains, and Julian Cheng, "*Wavelength Multiplexing and Demultiplexing using Multi-Wavelength VCSEL and Resonance-Enhanced Photodetector Arrays*", IEEE Photonics Technol. Lett., Vol. 10, no. 8, August 1998.

7) Yuxin Zhou, S. Luong, C.P. Hains, and Julian Cheng: "*Oxide-Confined Monolithic, Multiple-Wavelength Vertical-Cavity Surface-Emitting Laser Arrays with a 40 nm Wavelength Span*", IEEE Photonics Technol. Lett., Vol. 10, 1998.

8) Alduino, S. Q. Luong, Yuxin Zhou, C. P. Hains, and Julian Cheng, "*Quasi-Planar Monolithic Integration of High-Speed VCSEL and Resonant Enhanced Photodetector Arrays*", IEEE Photonics Technology Letters Vol. 11, no. 5, May 1999.

9) (Invited) Julian Cheng and Yuxin Zhou: "*High-Speed Wavelength Division Multiplexing and Demultiplexing Using Monolithic Integrated VCSEL and Resonant Photodetector Arrays*", IEEE Circuit and Device Magazine, Vol. 15, No. 6, pp. 17-27, Nov., 1999.

10) P. Hains, N.Y. Li, K. Yang, X.D. Huang, and Julian Cheng: "*Room-Temperature Pulsed Operation of Triple-Quantum Well GaInNAs/GaAs Lasers with Low Threshold Current Density Grown on Misoriented GaAs Substrates by MOCVD*", IEEE PhotonicsTechnol. Lett., Vol. 11, no. 10, pp. 1208-1210, October, 1999.

11) Kai Yang, C.P. Hains, and Julian Cheng: "*Room-temperature continuous-wave operation of a narrow-stripe oxide-confined GaInNAs/GaAs multi-quantum well laser grown by MOCVD*", IEEE Photonics Technol. Lett., Vol. 12, No. 1, pp. 7-9, Feb. 2000.

12) N. Y. Ki, C. P. Hains, Kai Yang, Jun Lu, P.W. Li, Julian Cheng: "*Organometallic vapor phase epitaxy growth and optical characteristics of almost 1.2 μm GaInNAs three-quantum-well laser diodes*", Applied Physics Letters, Vol. 75, no. 8, pp.1051-1053, 23 August, 1999.

13) Yuxin Zhou, Julian Cheng, and A. A. Allerman: "*High-Speed Wavelength Division Multiplexing and Demultiplexing Using Monolithic Quasi-Planar VCSEL and Resonant Photodetector Arrays with Strained InGaAs/GaAs Quantum Wells*," IEEE Photonics Technol. Lett., Vol. 12, No. 2, pp. , Feb. 2000.

14) Kai Yang, C.P. Hains, Julian Cheng, and A. A. Allerman: "*Efficient Double Intracavity-Contacted Vertical-Cavity Surface-Emitting Lasers with Very Low Threshold and Low Power Dissipation Designed for Cryogenic Applications*", IEEE Photonics Technol. Lett., Vol. 12, No. 2, pp., Feb. 2000.

15) Xiaodong Huang, A. Stintz, C. P. Hains, Julian Cheng, and K. J. Malloy. : "*Very Low Threshold Current Density Room Temperature Continuous-Wave Lasing from a Single-Layer InAs Quantum Dot Laser*", to be published in IEEE Photonics Technol. Lett., Vol. 12, No. 3, pp., Mar. 2000.

16) Kai Yang, Yuxin Zhou, X. D. Huang, C.P. Hains, and Julian Cheng, "*Monolithic, Oxide-confined, Multiple-Wavelength Vertical-Cavity Surface-Emitting Laser Arrays with a 57-nm Wavelength Grading Range using an Oxidized Upper Bragg Mirror*", IEEE Photonics Technol. Lett., Vol. 12, No. 4, pp., April, 2000.

17) Xiaodong Huang, A. Stintz, C. P. Hains, Julian Cheng, and K. J. Malloy : "*Efficient High-Temperature CW Lasing Operation of Oxide-Confined Long-Wavelength InAs Quantum Dot Lasers with Low Threshold Current Density*", Electronics Letters, Vol. 36, No. 1, pp. 41-42 , Jan. 6, 2000.

18) Yuxin Zhou, and Julian Cheng, "*1 Gb/s-per-channel Wavelength Division Multiplexed and Demultiplexing using Wavelength-Graded VCSEL And Resonance-Enhanced Photodetector Arrays*", to be published in IEEE Photonics Technol. Lett., Vol. 12, No. 6, 2000.

4.2. Conference Technical Papers:

1) Julian Cheng (Invited Paper): "*Reconfigurable Multi-Point Optical Interconnects using Vertical-Cavity Surface-Emitting Laser-Based Optoelectronic Switches Arrays*", Electrochemical Society Proceedings, Vol. 96-2, pp. 117-119, 1996.

2) Julian Cheng, Yin-Chen Lu, Bo Lu, and G. G. Ortiz, H. Q. Hou, J. C. Zolper, and M. J. Hafich, "*A New Optoelectronic Transceiver and Routing Switch Based on Vertical-Cavity Surface-Emitting Lasers, Photodetectors, and Heterojunction Bipolar Transisitors*", Proceeedings of SPIE, Vol. 3500-36, Feb. 1997.

3) Julian Cheng, S. Luong, G. G. Ortiz, Y. Zhou, J. Lu, C. P. Hains, H. Q. Hou, B. E. Hammons, G. A. Vawter: "*Monolithic Wavelength-Graded VCSEL and Wavelength-Selective Photodetector Arrays for WDM Applications,* SPIE Proceedings, Vol. 3290 "Integrated Optoelectronic Integrated Circuits II", pp. 123-129, 1998.

4) (Invited) Julian Cheng, S. Q. Luong, Y.-X. Zhou, A. C. Alduino, Jun Lu, C. P. Hains, H. Q. Hou, B. E. Hammons, G. A. Vawter: "*Monolithic wavelength-graded VCSEL and wavelength-selective photodetector arrays for wavelength-division-multiplexed optical interconnect applications,* SPIE Proceedings, Vol. 3288, "Optoelectronics Interconnects and Packaging V", pp. 2-9, Jan. 1998.

5) (Invited) Julian Cheng, Yuxin Zhou, S. Q. Luong, A. C. Alduino, and C. P. Hains: "*Wavelength-Division Multiplexed Optical Interconnects using Monolithic Wavelength-Graded VCSEL and Resonant Photodetector Arrays*", Proceedings of SPIE, Vol. 3627, Vertical-Cavity Surface-Emitting Lasers III, 1999.

6) (Invited Paper). Julian Cheng*, and Yuxin Zhou, "*High Speed Monolithic Integrated Optoelectronic Technologies for Wavelength Division Multiplexing and Demultiplexing Based on VCSELs*", Proceedings of SPIE Volume 3950-22, Optoelectronic Integrated Circuits IV, Jan. 2000.

7) (Invited Paper). Yuxin Zhou, and Julian Cheng: "*Gigabit-per-sec wavelength-division-multiplexed fiber-optic link*", Proceedings of SPIE Vol. 3949 – WDM and Photonic Switching Devices for Networking Applications", Jan. 2000.

4.3. Conference Presentations:

1) G.G. Ortiz, Julian Cheng, C. P. Hains, H. Q. Hou, J. C. Zolper, *"Monolithic Integration and Individually-Optimized Operation of $In_{0.2}Ga_{0.8}As$ Vertical-Cavity Surface-Emitting Lasers and Resonance Enhanced Quantum-Well Photodetectors"*, Conference Proceedings of the IEEE Laser and Electro-Optics Society, Vol. 2, pp. 273-274, 1996.

2) Julian Cheng, "MOCVD growth of monolithic, wavelength-chirped VCSELs and resonance-enhanced photodetector arrays", WOCSEMMAD 1997, San Antonio, Texas, Feb. 22, 1997.

3) G. G. Ortiz, S. Z. Sun and Julian Cheng, S. Z. Sun, H. Q. Hou,"*MOCVD Enhanced and Depleted Growth Rate Regions for Multiple Wavelength Vertical-Cavity Surface-Emitting Laser Arrays"*, CLEO 1997, May 1997.

4) G. G. Ortiz, S. Z. Sun and Julian Cheng, S. Z. Sun, H. Q. Hou,"*Monolithic Wavelength-Graded VCSEL and Resonance-Enhanced Photodetector Arrays for Parallel Optical Interconnects"*, LEOS 10th Annual Meeting Conference Proceedings, Vol. 2, Paper WJ-2, pp. 79-80; Nov. 1997.

5) Julian Cheng, S. Luong, G. G. Ortiz, Y. Zhou, J. Lu, C. P. Hains, H. Q. Hou, B. E. Hammons, G. A. Vawter: "*Monolithic Wavelength-Graded VCSEL and Wavelength-Selective Photodetector Arrays for WDM Applications"*, presented at the 1998 Photonics West Conference 3290, Integrated Optoelectronics, Jan. 28-30, San Jose, CA; 1998.

6) Julian Cheng, "Wavelength-division Multiplexing using monolithic VCSEL and Resonant Photodetector Arrays", 1998 Workshop on Semiconductor Materials and Devices", Feb. 23-25, 1998; Monterrey, CA.

7) Alduino, S. Luong, Yuxin Zhou, C. P. Hains, and Julian Cheng: " *Wavelength-Division Multiplexing and Demultiplexing using Monolithic Wavelength-Chirped VCSEL and Resonance-Enhanced Photodetector Arrays* ", 1998 CLEO Technical Digest , Vol. 6, pp. 367-368, 1998; Paper CThK2.

8) (Invited) Julian Cheng: "Monolithic, Wavelength-Graded, and Oxide-Confined VCSEL Arrays", Semiconductor Laser Workshop, San Francisco, CA, May 8, 1998.

9) (Invited Paper) Julian Cheng: "*Optical Multiplexing Technologies Based on VCSELs*", Invited aper presented at the La Jolla Advanced-Topics Research School Semiconductor Science and Technology Conference, Sept. 7-11, 1998; La Jolla, CA.

10) Yuxin Zhou, S. Luong, C.P. Hains, and Julian Cheng, "*Oxide-Confined Monolithic, Multiple-Wavelength Vertical-Cavity Surface-Emitting Laser Arrays with a 40 nm Wavelength Span"*, presented at the LEOS Annual Meeting, Dec. 4, 1998.

11) Julian Cheng: "*Room-Temperature Pulsed Lasing Operation of a GaInNAs/GaAs Multi-Quantum Well Laser Grown by MOCVD", and "Wavelength Division Multiplexing and Demultiplexing Using Monolithic Quasi-Planar VCSEL and Resonant Photodetector Arrays", two papers* presented at the Workshop on Compound Semiconductor Materials and Devices (WOCSEMMAD); New Orleans, LA; Feb. 22-24, 1999.

12) Alduino, S. Q. Luong, Yuxin Zhou, C. P. Hains, and Julian Cheng, "*A Quasi-Planar Approach to the Monolithic Integration of High-Speed VCSEL and Resonant Photodetector Arrays", and "*Conference on Lasers and Electro-Optics, Baltimore, MD; May 1999.

13) Julian Cheng, N.Y. Li, C. P. Hains, and K. Yang: "*Multi-Quantum Well GaInNAs/GaAs Lasers with Low Threshold Current Density Grown by MOCVD*", presented at the 57th Device Research Conference; Session VIIB; Santa Barbara, CA; June 28-30, 1999.

14) N. Y. Ki, C. P. Hains, Jun Lu, Kai Yang, Julian Cheng: "*Tellurium Memory Effects on OMVPE-Grown $In_{0.3}Ga_{0.7}As_{0.997}N_{0.003}$/GaAs Laser Diodes*", presented at the 41st Electronic Material Conference, Session G; Santa Barbara, CA; June 30-July2, 1999.

15) Yuxin Zhou, S. Q. Luong, and Julian Cheng*: "High-Speed Wavelength Division Multiplexing and Demultiplexing Using Monolithic Quasi-Planar VCSEL and Resonant Photodetector Arrays with Strained InGaAs/GaAs Quantum Wells*", 1999 LEOS Annual Meeting; San Francisco, CA: Nov., 1999.

16) Kai Yang, C. P. Hains, N.Y. Li, and Julian Cheng: "Near Room Temperature CW Lasing Operation of a Narrow-Stripe Oxide-Confined GaInNAs/GaAs Multi-Quantum Well Laser Grown by MOCVD,1999 LEOS Annual Meeting; San Francisco, CA: Nov., 1999

17) Kai Yang, C. P. Hains, and Julian Cheng, "*Efficient Above-Room-Temperature Continuous-Wave Operation of a GaInNAs/GaAs Multi-Quantum Well Laser Grown by MOCVD*", LEOS Summer Topical Meeting on VCSELs; San Diego, CA; July 28-30, 1999; post deadline paper PD-1.

18) Kai Yang, Yuxin Zhou, X.D. Huang, C.P. Hains, and Julian Cheng: "*Monolithic, Oxide-confined, Multiple-Wavelength Vertical-Cavity Surface-Emitting Laser Arrays with a very large wavelength grading span of 57-nm by using an Oxidized Upper Bragg Mirror*", to be presented in CLEO 2000; San Francisco, CA; May 2000.

19) Yuxin Zhou, and Julian Cheng: "*Gigabit-per-sec/channel Wavelength Division Multiplexed Optical Interconnect Using Multi-Wavelength VCSEL And Resonance-Enhanced Photodetector Arrays*" , ", to be presented in CLEO 2000; San Francisco, CA; May 2000.

20) Xiaodong Huang, A. Stingz, C. P. Hains, Julian Cheng, K. J. Malloy: *"Efficient high-temperature cw operation of oxide-confined long-wavelength InAs quantum dot lasers*", ", to be presented in CLEO 2000; San Francisco, CA; May 2000.

PAPERS:

1) G. G. Ortiz, S. Q. Luong, S. Z. Sun, and Julian Cheng, H. Q. Hou, G. A. Vawter, and E. Hammons: "*Monolithic, Multiple Wavelength Vertical-Cavity Surface-Emitting Laser Arrays by Surface-Controlled MOCVD Growth Rate Enhancement and Reduction*", IEEE Photonics Technol. Lett., Vol. 9, No. 8, pp. 1069-1071; August 1997.

2) G. G. Ortiz , C. P. Hains, S. Luong, S. Z. Sun, Julian Cheng, H. Q. Hou, G. A. Vawter and B. E. Hammons: *"Multiple Wavelength Vertical-Cavity Surface-Emitting Laser Arrays using Surface-Controlled MOCVD Growth Rate Enhancement and Reduction"*, OSA Trends in Optics and Photonics (TOPS), Vol. 15: Advances in Vertical-Cavity Surface-Emitting Lasers, edit. C.Chang-Hasnain, pp. 29-35, Sept. 1997.

3) S. Q. Luong, G. G. Ortiz, Y. Zhou, Jun Lu, C. P. Hains, Julian Cheng, H. Q. Hou, and G. A. Vawter: "*Monolithic, Wavelength-Graded VCSEL and Resonance-Enhanced Photodetector Arrays for Parallel Optical Interconnects*", IEEE Photonics Technol. Lett., Vol. 9, No. 5, pp. 642-644, May, 1998.

4) Julian Cheng, S. Luong, G. G. Ortiz, Y. Zhou, J. Lu, C. P. Hains, H. Q. Hou, B. E. Hammons, G. A. Vawter: "*Monolithic Wavelength-Graded VCSEL and Wavelength-Selective Photodetector Arrays for WDM Applications,* SPIE Proceedings, Vol. 3290 "Integrated Optoelectronic Integrated Circuits II", pp. 123-129, 1998.

5) (Invited) Julian Cheng, S. Q. Luong, Y.-X. Zhou, A. C. Alduino, Jun Lu, C. P. Hains, H. Q. Hou, B. E. Hammons, G. A. Vawter: "*Monolithic wavelength-graded VCSEL and wavelength-selective photodetector arrays for wavelength-division-multiplexed optical interconnect applications,* SPIE Proceedings, Vol. 3288, "Optoelectronics Interconnects and Packaging V", pp. 2-9, Jan. 1998.

6) Julian Cheng, Hao Zhu, Sanh Luong, and G. Simonis, " *Cryogenic VCSELS with Non-Uniform Multiple Quantum Wells for Parallel Optical Interconnects with a Wide Temperature Range of cw Operation*", Proceedings of the Sensors and Electron Device Symposium, pp. 49-53; Jan. 1998.

7) Alduino, Yuxin Zhou, S. Luong, C. P. Hains, and Julian Cheng, "*Wavelength Multiplexing and Demultiplexing using Multi-Wavelength VCSEL and Resonance-Enhanced Photodetector Arrays*", IEEE Photonics Technol. Lett., Vol. 10, no. 8, August 1998.

8) Yuxin Zhou, S. Luong, C.P. Hains, and Julian Cheng: "*Oxide-Confined Monolithic, Multiple-Wavelength Vertical-Cavity Surface-Emitting Laser Arrays with a 40 nm Wavelength Span*", IEEE Photonics Technol. Lett., Vol. 10, 1998.

9) Alduino, S. Q. Luong, Yuxin Zhou, C. P. Hains, and Julian Cheng, "*Quasi-Planar Monolithic Integration of High-Speed VCSEL and Resonant Enhanced Photodetector Arrays*", IEEE Photonics Technology Letters Vol. 11, no. 5, May 1999.

10) (Invited) Julian Cheng, Yuxin Zhou, S. Q. Luong, A. C. Alduino, and C. P. Hains: "*Wavelength-Division Multiplexed Optical Interconnects using Monolithic Wavelength-Graded VCSEL and Resonant Photodetector Arrays*", Proceedings of SPIE, Vol. 3627, Vertical-Cavity Surface-Emitting Lasers III, 1999.

Conference Papers:

1) Julian Cheng, S. Luong, G. G. Ortiz, Y. Zhou, J. Lu, C. P. Hains, H. Q. Hou, B. E. Hammons, G. A. Vawter: "*Monolithic Wavelength-Graded VCSEL and Wavelength-Selective Photodetector Arrays for WDM Applications",* presented at the 1998 Photonics West Conference 3290, Integrated Optoelectronics, Jan. 28-30, San Jose, CA; 1998.

2) (Invited paper) Julian Cheng, S. Q. Luong, Y.-X. Zhou, A. C. Alduino, Jun Lu, C. P. Hains, H. Q. Hou, B. E. Hammons, G. A. Vawter: "*Monolithic wavelength-graded VCSEL and wavelength-selective photodetector arrays for wavelength-division-multiplexed optical interconnect applications,* paper presented at the 1998 SPIE Conference (3288), Optoelectronics Interconnects and Packaging V, Jan. 28-29, 1998; San Jose, CA.

3) Alduino, S. Luong, Yuxin Zhou, C. P. Hains, and Julian Cheng: " *Wavelength-Division Multiplexing and Demultiplexing using Monolithic Wavelength-Chirped VCSEL and Resonance-Enhanced Photodetector Arrays* ", 1998 CLEO Technical Digest , Vol. 6, pp. 367-368, 1998; Paper CThK2.

4) Yuxin Zhou, S. Luong, C.P. Hains, and Julian Cheng, "*Oxide-Confined Monolithic, Multiple-Wavelength Vertical-Cavity Surface-Emitting Laser Arrays with a 40 nm Wavelength Span",* presented at the LEOS Annual Meeting, Dec. 4, 1998.

5) Alduino, S. Q. Luong, Yuxin Zhou, C. P. Hains, and Julian Cheng, "*A Quasi-Planar Approach to the Monolithic Integration of High-Speed VCSEL and Resonant Photodetector Arrays", and* "Conference on Lasers and Electro-Optics, Baltimore, MD; May 1999.

6) (Invited) Julian Cheng, Yuxin Zhou, S. Q. Luong, A. C. Alduino, and C. P. Hains: "*Wavelength-Division Multiplexed Optical Interconnects using Monolithic Wavelength-Graded VCSEL and Resonant Photodetector Arrays*", Photonics West Conference on Vertical-Cavity Surface-Emitting Lasers III, 1999.

7) Yuxin Zhou, S. Q. Luong, and Julian Cheng*: "High-Speed Wavelength Division Multiplexing and Demultiplexing Using Monolithic Quasi-Planar VCSEL and Resonant Photodetector Arrays with Strained InGaAs/GaAs Quantum Wells*", 1999 LEOS Annual Meeting; San Francisco, CA: Nov., 1999.